

An Actuation Model for Soft Robot Based on Amorphous Computational Material

Junqiang Wang

College of Physics and Electronic Information
Luoyang Normal University
Henan ,China
e-mail: wjq@lynu.edu.cn

Shuqiang Yang

College of Physics and Electronic Information
Luoyang Normal University
Henan ,China
e-mail: johnan@lynu.edu.cn

Changhong Yu

College of Physics and Electronic Information
Luoyang Normal University
Henan ,China
e-mail: yuchanghong@lynu.edu.cn

Jing Wu

College of Information Engineering
Henan University of Science and Technology
Henan ,China
e-mail: toya_2008@qq.com

Abstract—Amorphous Computational Material(ACM) is a concept of an active material that can sense its environment and, due to its cognitive capabilities, react “intelligently” to those changes. In such a material, we envision semiconducting polymer based sensing, actuation, and information process for on-board decision making to be combined into one active material. This paper describes incremental steps taken towards developing such a multifunctional active material with an intermediate goal of utilizing ACM as a “skin” of a soft robot –a robot, made of flexible materials, which is not bounded by its rigid structure and can adjust to its changing environment. We demonstrate the feasibility of utilizing water hammer as a form of directed actuation.

Keywords- *amorphous computational material ; soft robot ; actuation model*

I. INTRODUCTION

Current robotics systems have a limited capability to respond to contact (grasping, collision) with the environment. Some of the current solutions include torque sensors in the joints, external imaging and range sensors [1-3]. Amorphous Computational Material, or ACM, is a concept of an active material that has the capacity to sense its immediate environment and process that data for intelligent actuation –actuation where the applied force is based on the type of material handled. It will have the ability to sense forces acting upon it in 1D and 2D, and eventually even 3D, which later will be used to provide actuation in the same dimensions. An ACM will be fit with on-board information processing allowing for intelligent actuation that can be customized based upon the application and the operational environment. Because grasping a tomato requires different operational mode than tightening a metal bolt, ACM will allow for creating smart robotic actuators with the capacity to adjust grasping force for different objects. Other possible applications, including coating bridges with ACM, would provide information about cracks or

bulging of gusset plates allowing for proper authorities to be notified.

II. RESEARCH GOALS

In order to provide a feasibility study of the aforementioned Amorphous Computational Material our group is involved in a project aiming to create a soft robot where the ACM will be used as a “skin” for active interaction with its environment. Soft robots are a new group of mechanisms where their structure is not rigid but can adjust to the changing environment[4]. Commonly these systems are made from flexible materials, such as polymers. Semiconducting, conducting, and ferroelectric polymers have been used as piezoelectric sensors for strain gauges as well as actuators for contraction and expansion [5]. Also, a number of research groups have demonstrated complete robotics systems based in polymers [6-7]. Yeom et al., demonstrated a biomimetic jellyfish robot created with an ionic polymer metal composite that mimics the real loco motive behavior of a jellyfish. Sameoto, created an all-polymer foot capable of climbing walls, mimicking the ability of a gecko or spider foot. Both of these designs were inspired by biological systems. Polymer-based chemicals used as fuel [8] were developed in the mid-1990s, though they haven't gained much commercial success.

We envision our soft robot, made primarily from polymer components, to be propelled using a concept called water hammer (discussed later in the text) where ACM will be used to aid in steering. ACM will comprise of multiple cells where each cell has the following capabilities: sensing, actuation, cognition, and data transfer. Figure 1 demonstrates the concept of ACM. Sensing and actuation will be performed using polymer sensors and actuators. The data will be processed in a distributed fashion requiring distributed data processing algorithm as well as the capability for each cell to exchange the necessary information with other cells. For this data-processing task

we believe that a form of a neural network is perfectly suited as it naturally allows for data processing to be distributed and, in the case of individual ACM cells becoming non-operational, it does not result in a catastrophic failure [9].

We note that recently a number of research groups have demonstrated successful creation of “electronic skin” [10-11]. However, the proposed designs concentrate only on the sensing ability of their material and do not address cognition nor actuation aspects. As such our proposal differs starkly with the aforementioned designs.

This paper addresses the all-polymer, distributed cognition aspect of ACM cells as well as the actuation of the soft robot that the ACM will be used with. ACM polymer sensors and actuators, and wireless data communication are part of our long-term vision, but are not addressed in here.

Our ACM will be used as a “skin” for our soft robot that will allow it to intelligently interact to the changes to its environment. The soft robot, however, will be actuated externally through a phenomenon known as water hammer, which is discussed next.

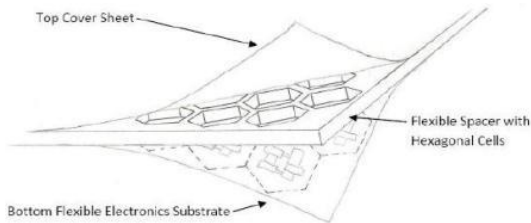


Figure 1. Proposed ACM architecture. Each cell, neighboring with 6 cells, will be equipped with a polymer micro sensor and actuator as well as distributed cognition (SNN).

III. WATER HAMMER

The water hammer effect, also known as fluid hammer, has been known since the introduction of the modern plumbing. Until recently it was viewed as a negative effect with capacity to destroy indoor and outdoor plumbing and, as a result, a number of remedies were developed to mitigate its effects. This phenomenon occurs when water traveling through a pipe experiences a rapid and sharp change in pressure usually facilitated by a fast closure of a valve. Increase in pressure, at the point of the closure, is brought about by the continuous motion of the flowing liquid. The intensity of the water hammer effect is inversely proportional to the time in which the valve is closed: the shorter the shutoff time the greater the force of the effect.

Recently Perrin et al. [12] demonstrated the feasibility of harnessing this potentially devastating effect towards a useful application. In their experiment a wheeled object was placed at the end of a tether which featured a looped hose with a shutoff valve, see Figure 2. The object was a remotely operated car with a small electric engine. Increasing the length of the tether resulted in increased weight which eventually presented a difficulty for the car to pull. The main challenge of the task occurred when the tether was placed in a situation that resulted in the tether

being stuck. Following Perrin’s work, we conducted two experiments; one with the tether wrapped around two cylindrical objects, forming an S curve, and the second with the tether being stuck underneath a door. In both situations the jittery movement of the hose, caused by the water hammer effect, resulted in the tether being set loose enough for the small car to pull it.

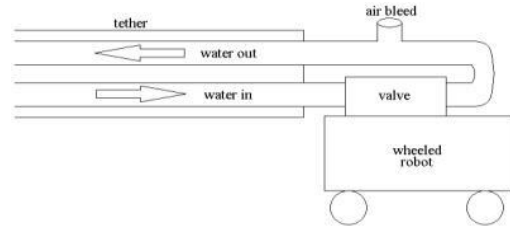


Figure 2. Design diagram of water hammer experiment

A second set of experiments was aimed at identifying if the water hammer effect could be used as an exclusive source of actuation. The experiment demonstrated that, with a straight hose, the cart would be propelled directly along the length of the hose. We also conducted a drag test, in which a weight was placed on top of one tether with no water hammer and on top of a second tether aided by the water hammer effect. The conclusion was that the tether aided by the water hammer effect was able to pull a weight almost twice that of the unaided tether. For more in-depth experimental set up and results please see [23-24].

IV. DIRECTED PROPULSION

Based upon the observation that water hammer actuation is effective as a sole source of propulsion along a straight line, our team investigated the following hypothesis: can we affect direction of motion of a robot placed at the end of a hose, by varying the hose’s shape and applying the water hammer effect.

A. Computer Simulation

We constructed a computer simulation of the resultant force vector due to the shape of the hose, acting on the front-mounted object. For the purposes of the simulation, the hose was considered to comprise of a finite number of elements, each in direct contact with adjacent elements. Each finite element had a point placed at its center. These individual points were connected, in the XY-Plane, resulting in an

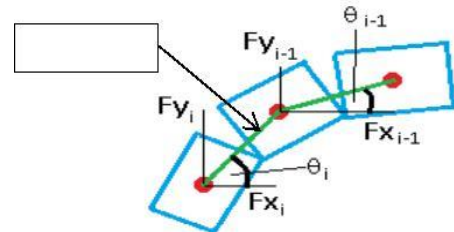


Figure 3. Finite elements used to describe the serpentine shape of the hose, along with their corresponding F_x and F_y components. The measured angles are analogous to the information collected by the bend sensors.

approximate representation of the shape based on the formed angles, measured in radians. These angles

measured are analogous to the information collected by bend sensors placed along the length of the hose, which will be used to represent its shape. Figure 3 illustrates the concept.

For the 0th order of approximation the angles (θ in Figure 3) were summed up resulting in unique angles for individual shapes. For the 1st order of approximation the last element (the furthest away from the valve) was assigned X and Y components of the aforementioned angle. Each subsequent element (closer to the valve) had its force calculated based on its X and Y components with a scaled force of the previous component added. The scaling factor d , left as a variable, was adjusted through various trials, between values of „0“ and „1“. Increasing the scaling factor corresponded to an increase in the influence of the previous component(s). Equations 1 and 2 show the formulae used to calculate the individual force components.

$$Fx_i = \cos(\theta_i) + d * Fx_{i-1} \quad (1)$$

$$Fy_i = \sin(\theta_i) + d * Fy_{i-1} \quad (2)$$

TABLE I. RESULTANT VECTORS DISTINCT WITH DIFFERENT D VALUE(COMPUTER SIMULATION)

Shape	0 th order	1 st order						
		d=0	d=0.1	d=0.2	d=0.3	d=0.5	d=0.8	d=1
1	-0.1	2.4	2.4	2.5	2.6	2.8	2.9	3
2	0	1.6	1.6	1.6	1.6	1.6	1.9	2.8
3	0.5	-2.5	-2.5	-2.5	-2.5	-2.6	-3	2.1
4	0.4	2.4	2.4	2.4	2.5	2.5	2.7	2
5	0.3	1.2	1.2	1.2	1.2	1	0.7	1.3
6	-0.2	-0.4	-0.4	-0.4	-0.4	-0.4	-0.5	-1
7	-0.3	-2.4	-2.4	-2.4	-2.4	-2.4	-2.5	-3
8	-0.1	2.9	2.9	2.9	2.9	3	3.1	-3.1
9	1	0.4	0.4	0.4	0.5	0.5	0.4	0.5
10	-0.6	2.7	2.7	2.7	2.7	2.7	3	-2.4
11	-1.4	-0.5	-0.5	-0.5	-0.6	-0.8	-1.4	-1.4
12	-1.3	-0.5	-0.5	-0.5	-0.6	-0.8	-1.2	-1.4
13	-0.5	-1.4	-1.4	-1.4	-1.4	-1.4	-1.3	-1.2
14	0.4	2.7	2.6	2.6	2.5	2.4	2	1.1
15	-0.1	0.8	0.8	0.8	0.8	0.8	0.7	-0.1
16	1.3	0.8	0.8	0.8	0.8	0.8	1	1.3
17	1.7	2.4	2.4	2.4	2.4	2.3	2.1	1.8
18	1.3	0	0	0	0.1	0.2	0.9	1.4
19	1	0	0	0	0.1	0.2	0.8	1.2
20	-0.3	-0.9	-0.9	-0.9	-1	-1	-1.2	-0.5
21	1.2	0	0	0	0	0	0.3	1.3
22	1.1	0	0	0	0	0.1	0.5	1.2

Table I shows the obtained resultant vectors for 22 distinct shapes for both 0th and 1st order of approximation with varying d factor (values for resultant force vector are given in radians). Analysis of Table I reveals that increasing d from „0“ to „0.2“ does

not produce a noticeable change in the vector. However, as d is increased beyond „0.5“, some of the shapes result in significantly varying vectors. This is greatly in line with the expectation that increasing the influence of individual elements will result in a greater change in the force acting on the front-mounted valve. Intuitively extreme values, $d=0$ and $d=1$, are non-realistic values and a value somewhere between those extremes should the most closely relate to real conditions.

B. Experimental Setup

The most realistic value of the d factor (from section Computer Simulation), however, can only be evaluated empirically by comparing the results from the computer simulation to the results obtained in a practical experiment. Hence, the next thing that needed to be done was to experimentally obtain the data relating the shape of the hose to the force acting on the valve. We attached the valve to a stationary (mounted to a large metal plate) force sensor that would measure the force impacting on the valve through the water hammer, in the X and Y direction. The sensor registers force in X, Y, and Z directions. We disregarded the Z direction as the tube existed in a planar space. For more details about experimental setup please see[13].

TABLE II. FITTING RESULTANT VECTORS

Shape	WH Exp	1 st order					
		d=0	error	d=0.1	error	d=0.5	error
0	1.57	1.57	0%	1.57	0%	1.57	0%
1	1.61	1.55	3%	1.57	2%	1.64	2%
2	1.66	1.5	9%	1.54	7%	1.82	9%
3	1.64	1.5	9%	1.52	7%	1.38	16%
4	1.73	1.52	12%	1.55	10%	1.73	0%
5	1.54	1.4	9%	1.41	8%	1.55	1%
6	1.2	1.27	6%	1.26	4%	1.33	10%
7	1.15	1.36	18%	1.33	15%	1.26	9%
8	1.05	1.34	28%	1.31	25%	1.33	27%
9	1.52	1.38	9%	1.34	11%	1.15	24%
10	1.73	1.8	4%	1.87	8%	2.16	25%
11	1.48	1.4	6%	1.33	11%	0.93	38%
12	1.17	1.19	1%	1.13	3%	1.01	13%
13	1.52	1.5	1%	1.5	1%	1.48	2%
14	1.55	1.59	2%	1.59	2%	1.59	2%
15	1.55	1.5	3%	1.52	2%	1.55	0%
16	1.41	1.38	2%	1.34	5%	1.17	17%
17	1.71	1.83	7%	1.83	7%	1.99	16%
18	1.73	1.64	5%	1.62	6%	1.73	0%
19	1.45	1.57	8%	1.57	8%	1.47	1%
Average error			7.10%		7.10%		10.60%

The experiment included measurement of 20 distinct shapes. For each of the shapes, the resultant force vector, obtained by extracting point(s) of the greatest magnitude (in XY plane) of all of the impacting forces recorded, was matched with 20 distinct points on the hose that were obtained from pictures taken of the shape (analogous to information collected by bend sensors) before the application of the water hammer (throughout the experiment the shape would slightly

change due to the forces generated by the effect). Figure 4 demonstrates an example shape used for this experiment. Table II presents the data obtained, with 20 different shapes each with a distinct force vector (the values are given as the angle, in radians, calculated from the X axis in the counter-clockwise direction). Shape 0 is a reference shape, where the hose does not have any bends and the angle equals to $\pi/2$.

V. COMPARISON OF SIMULATION AND EXPERIMENTAL DATA

In order to verify the accuracy of our computer simulation (see section Computer Simulation) we used the shape data obtained during the lab experiment and matched it with our resultant force vector from the simulation. This fitting process involved modifying the parameter d in Eq. 1 and 2 (the influence of individual finite elements on consecutive elements) until the difference was satisfactorily small.

TABLE III. COMPARISON OF RESULTANT VECTORS OBTAINED WITH HOSE SHAPES RESULTING FROM DENSER POINTS(1,2,3,4)AND SPARSER POINTS(1,5,9,14)

Shape	WH Exp	1 st order					
		1, 2, 3, 4	error	1, 3, 5, 7	error	1, 5, 9, 14	error
0	1.57	1.57	0.00%	1.57	0.00%	1.57	0%
1	1.61	1.57	2.48%	1.57	2.48%	1.57	2%
2	1.66	1.54	7.23%	1.57	5.42%	1.61	3%
3	1.64	1.52	7.32%	1.48	9.76%	1.43	13%
4	1.73	1.55	10.40%	1.57	9.25%	1.57	9%
5	1.54	1.41	8.44%	1.43	7.14%	1.43	7%
6	1.2	1.26	5.00%	1.27	5.83%	1.33	11%
7	1.15	1.33	15.65%	1.33	15.65%	1.34	17%
8	1.05	1.34	27.62%	1.34	27.62%	1.36	30%
9	1.52	1.34	11.84%	1.33	12.50%	1.33	13%
10	1.73	1.87	8.09%	1.88	8.67%	1.87	8%
11	1.48	1.33	10.14%	1.31	11.49%	1.31	11%
12	1.17	1.13	3.42%	1.15	1.71%	1.19	2%
13	1.52	1.5	1.32%	1.64	7.89%	1.64	8%
14	1.55	1.59	2.58%	1.59	2.58%	1.59	3%
15	1.55	1.52	1.94%	1.52	1.94%	1.52	2%
16	1.41	1.34	4.96%	1.34	4.96%	1.33	6%
17	1.71	1.83	7.02%	1.85	8.19%	1.88	10%
18	1.73	1.62	6.36%	1.64	5.20%	1.68	3%
19	1.45	1.57	8.28%	1.55	6.90%	1.68	16%
Average error			7.50%		7.76%		8.61%

Table II presents data calculated for three different values of d factor equal to „0“, „0.1“, and „0.5“. It can be seen that, for d=0.1, the average error is the smallest, or 7.2% (we also measured the error for values slightly higher and lower than 0.1 but the error was greater in both cases). However, for d=0.5 error increases to about 10.7%. This finding indicates that the direction of propulsion is only mildly affected by the overall shape of the hose and the greatest influence is due to the direction or shape of the very

end of the hose. In the future we plan to investigate if our results would change when the water hammer effect is altered, either by increasing or decreasing it (facilitated by changes in the diameter of the hose or the water pressure).

VI. CONCLUSION

To further verify the greater importance of points that are the closest to the front-mounted valve as opposed to points further away from the valve, we repeated the comparison of the computer simulation with the experimentally obtained values. This time we only included four points as opposed to 20 points. We compared information obtained from points numbered 1,2,3,4 with that of 1,3,5,7 and 1,5,9,14 (point no. 1 was the first point after the valve). The d factor was held fixed at „0.1“. Table III demonstrates our findings. It can be seen that spacing the points (equivalent with placing the bend sensors) closest to the front-mounted valve results in the closest approximation of the resultant force, or 7.4%. It should be noted that, even though the accuracy of simulation with four points is comparable to 20 points, accuracy suffers slightly when the overall number of measurements is reduced (7.4% vs 7.2%).

The conclusion of our experiments is that we have three different sources of information that all lead in the same direction. This, we believe, validates our assumptions.

ACKNOWLEDGMENT

This work was financially supported by Science and technology key research projects of department of Henan province education (14A510012) , Application Fund Project of Luoyang Normal University (No. 2013-YYJJ-001). science and technology development project of Department of henan province(142102210572).

REFERENCES

- [1] K. Harada, F. Kanehiro, G. Miyamori, K. Akachi, "Humanoid Robot HRP-3", Proc. of 2008 IEEE IROS.
- [2] D. Fioravanti, B. Allotta, A. Rindi, "Image based visual servoing for robot positioning tasks," *Meccanica*, Vol. 43, pp 291-305, 2008.
- [3] D. R. Frutiger, B. E. Kratochvil, B. J. Nelson, "Magmites – microrobots for Wireless Microhandling in Dry and Wet Environments – Video Submission", Proc. of 2010 IEEE ICRA.
- [4] A. Albu-Schaffer, O. Eiberger, M. Grebenstein, S. Haddain, C. Ott, T. Wimbock, S. Wolf, G. Hirzinger, "Soft robotics," *IEEE Robotics & Automation Mag.*, Vol. 15, no. 3, pp. 20-30, 2008.
- [5] J. Lu, S.G. Kim, S. Lee, I.K. Oh, "Fabrication and actuation of electro-active polymer actuator based on PSMI-incorporated PVDF," *Smart Materials & Structures*, Vol. 17, Issue 4, Aug 2008.
- [6] S.W. Yeom, I.K. Oh, "A biomimetic jellyfish robot based on ionic polymer metal composite actuators," *Smart Materials & Structures*, Vol 18, Issue 8, Aug 2009.
- [7] D. Sameoto, Y.S. Li, C. Menon, "Multi-scale Compliant Foot Designs and Fabrication for Use with a Spider-Inspired Climbing Robot," *Journal of Bionic Engineering*, Vol. 5, Issue 3, Pg 189-196, Sept 2008.
- [8] M. Nagao, S. Jayaram, M. Sugio, E. P. Waldi, "Studies on the dielectric strength of oil-polymer composite insulation under variable frequency AC voltages," *Electrical Insulation and Dielectric Phenomena*, 1999 Ann Rep Con, Vol. 1, pp 309-312.

- [9] R. A. Nawrocki, M. Shaalan, R. M. Voyles, "Monitoring Artificial Neural Network Performance Degradation Under Network Damage," to appear in proceedings of ANNIE 2010.
- [10] S. C. B. Mannsfeld, B. C-K. Tee, R. M. Stoltenberg, C. V. H-H. Chen, S. Barman, B. V. O. Muir, A. N. Sokolov, C. Reese, Z. Bao, "Highly sensitive flexible pressure sensors with microstructured rubber dielectric layers," *Nature Materials*, Pub. Online: 12 Sept 2010.
- [11] K. Takei, T. Takahashi, J. C. Ho, H. Ko, A. G. Gillies, P. W. Leu, R. S. Fearing, A. Javey, "Nanowire active-matrix circuitry for low-voltage macroscale artificial skin," *Nature Materials*, Pub. Online: 12 Sept 2010.
- [12] R. L. Feller, D. P. Perrin, R. D. Howe, "Validation and Explanation of Waterhammer-Based Locomotion," *Robotics and Automation*, 2006, ICRA, pp 4264-4269.
- [13] X. Yang, R. Voyles, K. Li, "Experimental Comparison of Robotics Locomotion with Passive Tether and Active Tether," to appear in Proceedings of the 2009 IEEE International Workshop on Safety, Security, and Rescue Robotics, 2009.